Infrared constrained equilibrium reconstruction and application to snowflake divertor studies

by

J.T. Wai

with

P.J. Vail, A.O. Nelson, Z.A. Xing,
C. Lasnier, E. Kolemen

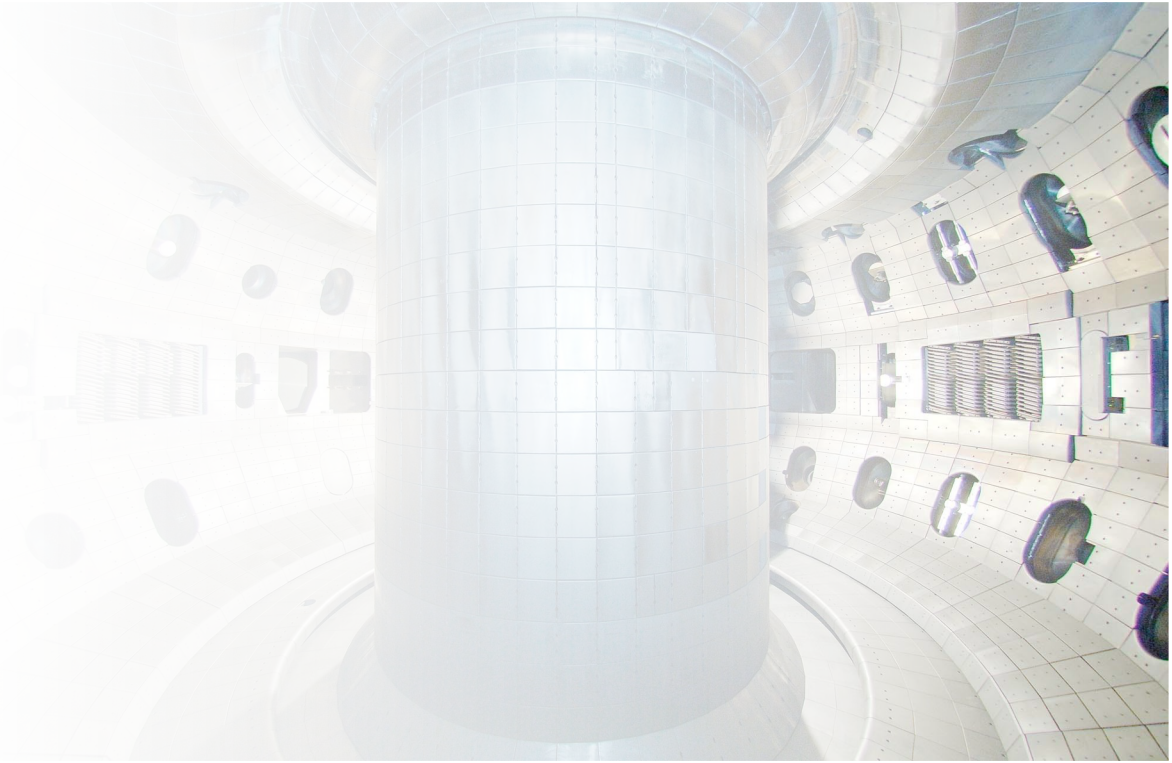

APS – DPP 2020

Nov 10, 2020

Equilibrium geometry is difficult to resolve in advanced divertors

- Some advanced divertors (e.g. snowflake, x-divertor, nearby-double-null) introduce another x-point into the divertor region.
- At the x-point, $\nabla\psi = B_p = 0 \Rightarrow$ there is a large region of low magnetic field. Equilibrium geometry is sensitive to external measurements and variations from the Grad-Shafranov equation.
- Divertor heat flux $\mathbf{q}_\perp$ measured from infrared-thermography (IRTV) diagnostic inconsistent with equilibrium.

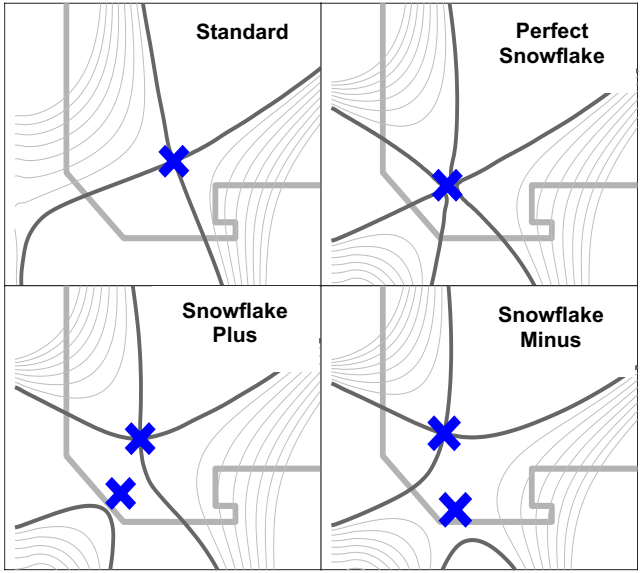

IRTV diagnostic can be used to resolve inconsistencies in the snowflake divertor equilibrium

- **Snowflake plus:** secondary x-point lies in the *private flux region*. Scrape-off layer (SOL) fieldlines directly intersect divertor in 2 locations ⇒ 2 heat flux peaks.
- **Snowflake minus:** secondary x-point lies in the SOL. Fieldlines directly intersect divertor in 3 locations ⇒ 3 heat flux peaks.
- Equilibrium vs. IRTV inconsistencies
  - Strike point location mismatch
  - Occasionally, incorrect # of heat flux peaks for the snowflake type
- IRTV used to improve equilibrium
  - Useful for control (feedback on x-point locations [Kolemen, 2018])
  - Geometry sensitive to unmeasured divertor currents. Potential use as diagnostic for bootstrap current.

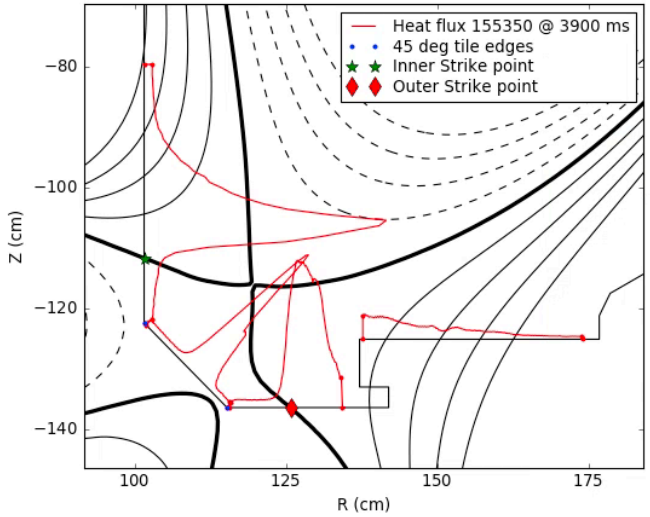

EFIT01 indicates SFD+, but 3 heat flux peaks (SFD-)

Algorithm developed to infer SFD x-point locations from IRTV characteristics

- **Snowflake minus:** 4 quantities are derived from heat flux profile: 3 strike points + flux coordinate of secondary x-point ψ_{xp2}
- Used to match 4 degrees of freedom in x-points: (r,z) at 2 x-points
- "True" strike points identified from fit to Eich profile [Eich, 2013]

$$q(\bar{s}) = \frac{q_0}{2} \cdot \exp\left(\left(\frac{S}{2\lambda_q}\right)^2 - \frac{\bar{s}}{\lambda_q \cdot f_x}\right) \cdot \operatorname{erfc}\left(\frac{S}{2\lambda_q} - \frac{\bar{s}}{S \cdot f_x}\right)$$

$$\bar{s} = s - s_0$$

- **Snowflake plus:** similar procedure but less information available. See [Wai, 2020] for details.

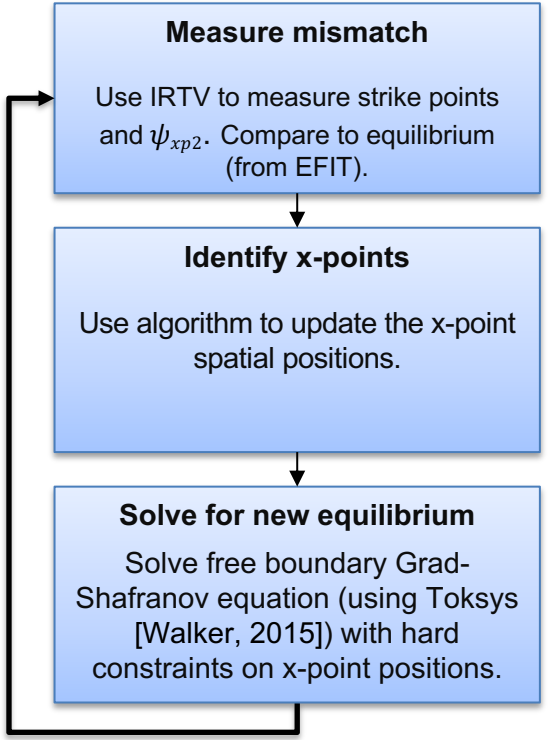

~4-5 iterations to converge

Outboard power fraction identifies midplane radial coordinate for the secondary separatrix

- At midplane, exponentially decaying heat flux
- Midplane radius of secondary separatrix $r_{mid,xp2}$ related to the power splitting in the 2 outboard SFD-minus heat peaks.
- However, first need to measure the $\lambda_{q,eff}$ for power splitting which is 2-3x larger than λ_q from Eich. [Maurizio, 2018]

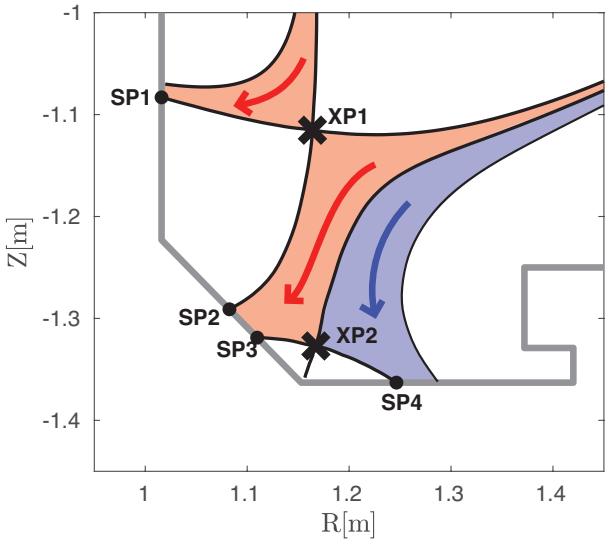

$$f_{sp4} := \frac{P_4}{P_2 + P_4} = \frac{\int_{r_{mid,xp2}}^{\infty} q_{\perp}^{mid,peak} e^{-r/\lambda_q^{eff}} dr}{\int_0^{\infty} q_{\perp}^{mid,peak} e^{-r/\lambda_q^{eff}} dr} = e^{-r_{mid,xp2}/\lambda_q^{eff}}$$

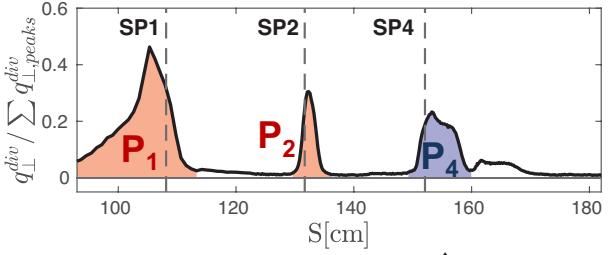

$\lambda_{q,eff}$ measured by fitting power fraction to multiple equilbria

- Power fraction f_{sp4} measured from the divertor heat flux profile. At each peak, $P_{pk} = \int 2\pi R(s) q_{\perp}(s) ds$
- Secondary separatrix position $r_{mid,\,xp2}$ measured from EFIT equilibrium.
- Data is selected from subset of shots that have wide range of x-point separation and fit to:

$$f_{sp4} = e^{-(r_{mid,xp2}+\epsilon)/\lambda_q^{eff}}$$

- ϵ is a fitting parameter to account for systematic bias in the reconstruction
- $\lambda_{q,eff}$ = 5.6mm versus λ_q = 1.9mm from Eich fit

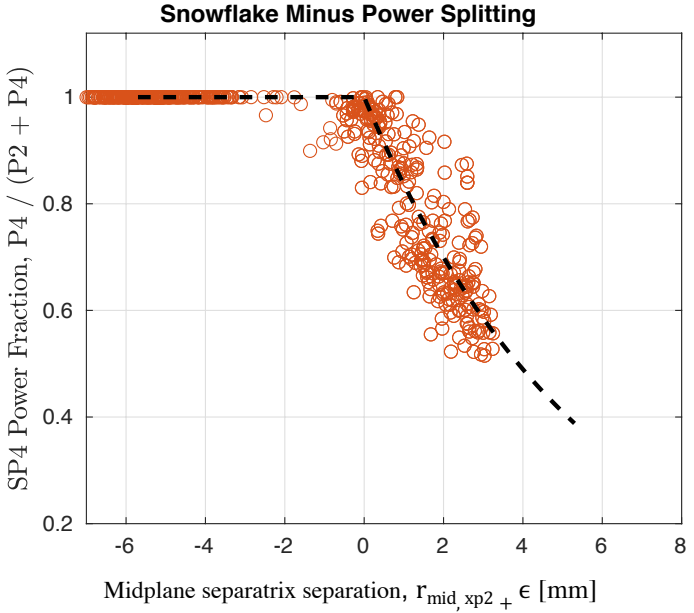

Algorithm converges and simulations match heat profile

- Simple assumptions and geometry used to update x-point positions. See [Wai, 2020] for derivation.

$$\Delta x\vec{p}_1 = \text{sign}(\langle \vec{e_1}, \hat{N}_{xp1} \rangle)|\vec{e_1}|\hat{N}_{xp1} + \text{sign}(\langle \vec{e_2}, \hat{E}_{xp1} \rangle)|\vec{e_2}|\hat{E}_{xp1}$$

$$\Delta x\vec{p}_2 = \text{sign}(\langle \vec{e_4}, \hat{N}_{xp2} \rangle)|\vec{e_4}|\hat{N}_{xp2} + f_x \Delta r_{split} \hat{E}_{xp2}$$

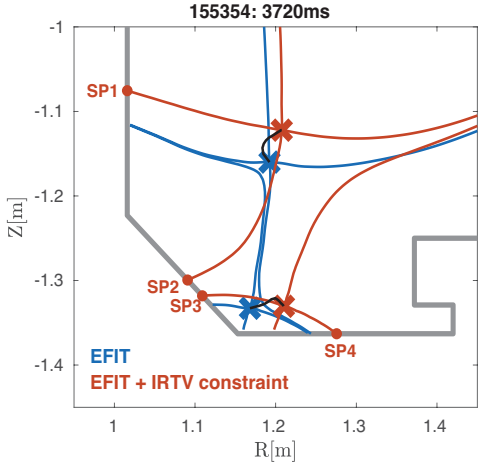

- **Example:** EFIT01 equilibrium indicates SFD-plus, but 3 heat flux peaks indicates SFD-minus.
- Converged equilibrium is SFD-minus
- Simulated heat flux, obtained using SFD power flux model [Vail, 2019], agrees with IRTV.

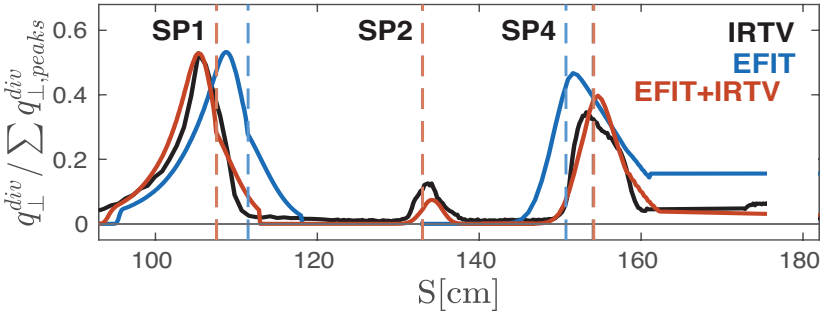

Preliminary: bootstrap current decreases ~16% to match new equilibrium shape.

- Unmeasured divertor currents can alter divertor flux surfaces significantly [Ryutov, 2010] ⇒ potential to use change in flux surfaces from IRTV to infer these currents.
- SFD algorithm performed on kinetic equilibria obtained from CAKE [Xing, 2020].
- Preliminary: 16% reduction in edge current due to shape change.
  - Need to incorporate algorithm directly into kinetic solvers (vice TokSys)
  - Not all available diagnostics used for fit.
- Edge current reduction linearly correlated with change in x-points.

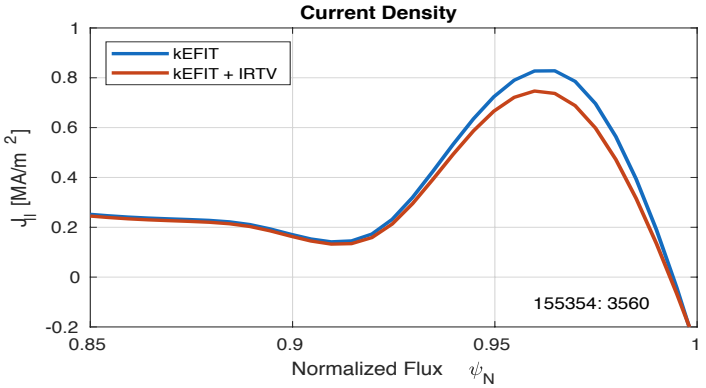

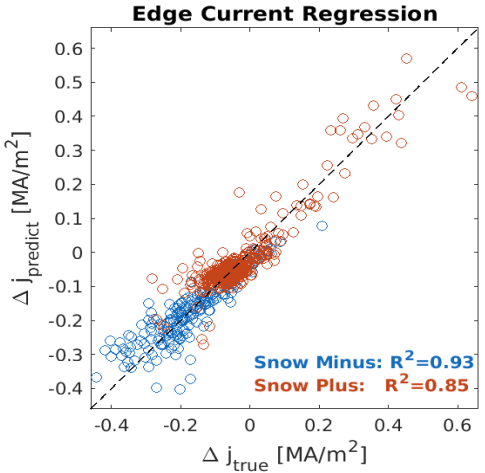

IRTV constraint must be balanced against other diagnostics

- Algorithm can be used as a virtual diagnostic for x-point positions. However, must balance this against other equilibrium diagnostics.
- **Fitting trade-off example:** 155354
  - Original eq is SFD-plus, but IRTV shows 3 peaks (SFD-minus)
  - Fitting weight is applied to x-point constraint (Δxp driven to zero)
  - wt=0.45, equilibrium prediction is SFD-minus. B-probe error increased by 30%.
  - wt=1.0, Δxp driven to zero. Strike point and flux errors concurrently become zero. But B-probe error has increased by 2.5x

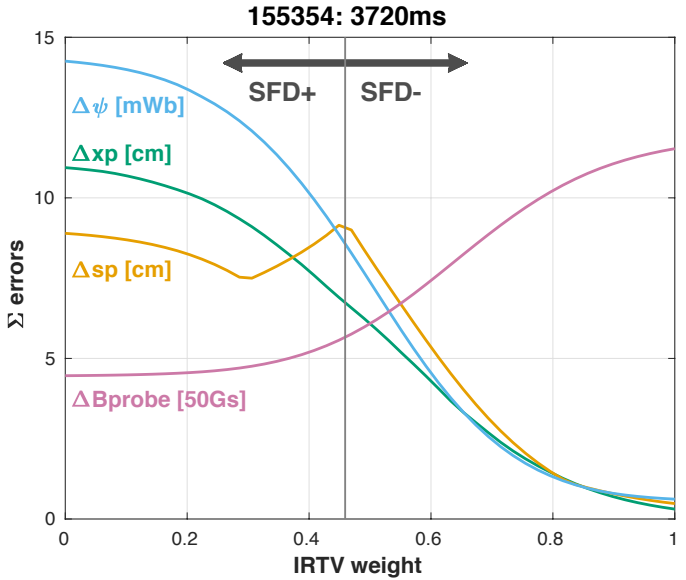

Δxp	Δsp	$\Delta\psi$	B-probe
Summed mismatch in x-point positions, desired vs. equilibrium	Summed mismatch in strike point positions, IRTV vs equilibrium	Flux coordinate of the secondary separatrix, desired vs. equilibrium	Summed errors in magnetic probes, measured vs. fit

DIII-D NATIONAL FUSION FACILITY

Future Work

- Incorporate algorithm directly into EFIT / kinetic EFIT codes for higher confidence in edge current modifications
- DIII-D may develop real-time 1D heat flux capabilities ➔ use for advanced divertor control.

References

T. Eich, et al., “Scaling of the tokamak near the scrape-off layer H-mode power width and implications for ITER”, NF, 2013.

E. Kolemen, et al., “Initial development of the DIII–d snowflake divertor control” NF, 2018.

R. Maurizio, et al., “The effect of the secondary x-point on the scrape-o layer transport in the TCV snowake minus divertor”, NF, 2018.

P. Vail, et al., “Optimization of the snowflake divertor for power and particle exhaust on NSTX-U”, NME, 2019.

D. D. Ryutov, et al., “Local properties of the magnetic field in a snowflake divertor”, PPCF, 2010.

J.T. Wai, et al., “Infrared constrained equilibrium reconstruction and application to snowflake divertor studies”, NME, 2020. Accepted.

M. L. Walker, et al., “Development environments for tokamak plasma control”, IEEE SOFE, 2015.

Acknowledgements: This material is based upon work supported by the U.S. Department of Energy, Office of Science, Office of Fusion Energy Sciences, using the DIII-D National Fusion Facility, a DOE Office of Science user facility, under Awards DE-FC02-04ER54698, DE-AC02-09CH11466, DE-SC0015878, and DE-AC52-07NA27344.

Backup

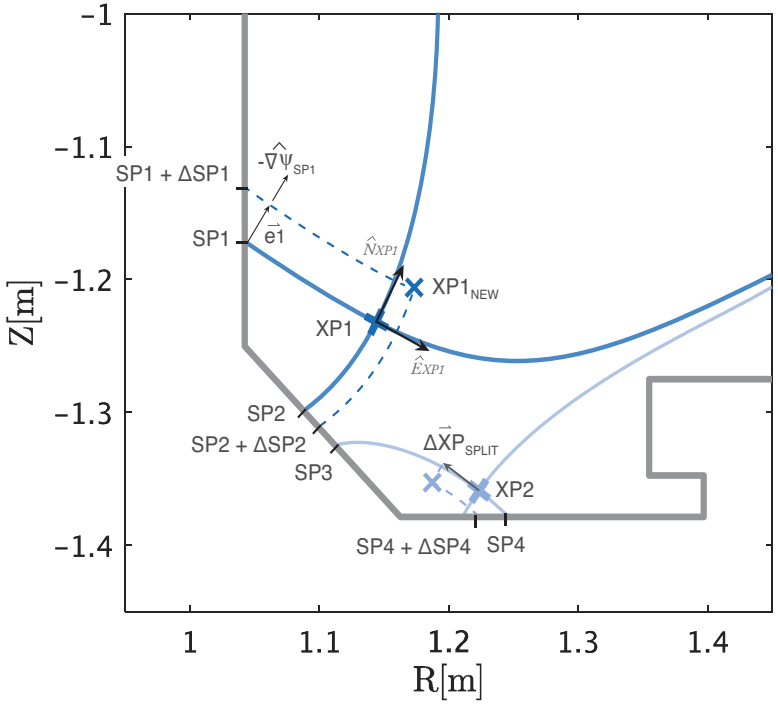
-1
-1.1
-1.2
-1.3
-1.4
Z[m]
1
1.1
1.2
1.3
1.4
R[m]
SP1 + ΔSP1
SP1
$-\hat{\nabla}\hat{\psi}_{SP1}$
$\vec{e1}$
$\hat{N}_{XP1}$
$XP1_{NEW}$
XP1
$\hat{E}_{XP1}$
SP2
SP2 + ΔSP2
SP3
$\Delta\vec{X}P_{SPLIT}$
XP2
SP4 + ΔSP4
SP4